Acta Cryst E CRYSTALLOGRAPHIC COMMUNICATIONS

ISSN 2056-9890

The first coordination compound of deprotonated 2-bromonicotinic acid: crystal structure of a dinuclear paddle-wheel copper(II) complex

Nives Politeo,[a] Mateja Pisačić,[b] Marijana Đaković,[b] Vesna Sokol[a]* and Boris-Marko Kukovec[a]

[a]Department of Physical Chemistry, Faculty of Chemistry and Technology, University of Split, Ruđera Boškovića 35, HR-21000 Split, Croatia, and [b]Department of Chemistry, Faculty of Science, University of Zagreb, Horvatovac 102a, HR-10000 Zagreb, Croatia. *Correspondence e-mail: vsokol@ktf-split.hr

Received 19 December 2019
Accepted 13 January 2020

Edited by W. T. A. Harrison, University of Aberdeen, Scotland

Keywords: crystal structure; copper(II); 2-bromonicotinic acid; dinuclear paddle-wheel cluster; hydrogen-bond motif.

CCDC reference: 1977430

Supporting information: this article has supporting information at journals.iucr.org/e

A copper(II) dimer with the deprotonated anion of 2-bromonicotinic acid (2-BrnicH), namely, tetrakis(μ-2-bromonicotinato-κ^2O:O')bis[aquacopper(II)]-(*Cu*—*Cu*), $[Cu_2(H_2O)_2(C_6H_3BrNO_2)_4]$ or $[Cu_2(H_2O)_2(2\text{-Brnic})_4]$, (**1**), was prepared by the reaction of copper(II) chloride dihydrate and 2-bromonicotinic acid in water. The copper(II) ion in **1** has a distorted square-pyramidal coordination environment, achieved by four carboxylate O atoms in the basal plane and the water molecule in the apical position. The pair of symmetry-related copper(II) ions are connected into a centrosymmetric paddle-wheel dinuclear cluster [Cu···Cu = 2.6470 (11) Å] *via* four *O*,*O*′-bridging 2-bromonicotinate ligands in the *syn-syn* coordination mode. In the extended structure of **1**, the cluster molecules are assembled into an infinite two-dimensional hydrogen-bonded network lying parallel to the (001) plane *via* strong O—H···O and O—H···N hydrogen bonds, leading to the formation of various hydrogen-bond ring motifs: dimeric $R_2^2(8)$ and $R_2^2(16)$ loops and a tetrameric $R_4^4(16)$ loop. The Hirshfeld surface analysis was also performed in order to better illustrate the nature and abundance of the intermolecular contacts in the structure of **1**.

1. Chemical context

Copper(II) carboxylates have been studied extensively because of their structural diversity and related possible applications. The origin of this diversity is in the variable donating ability of the carboxylate oxygen atoms and in the nature of the other coordinated ligands (Iqbal *et al.*, 2013; Song *et al.*, 2009). The structural diversity of copper(II) carboxylates depends strongly on the inclusion of additional coligands (*e.g.* hydroxy, alkoxy and azide ions), which are able to mediate magnetic coupling between the copper(II) ions and to enable ferromagnetic and antiferromagnetic interactions *via* their various bridging modes (Zhang *et al.*, 2012; Ma *et al.*, 2014).

Copper(II) carboxylates can find applications as biologically active agents (Fountoulaki *et al.*, 2011; Lim *et al.*, 2009), as electrochemical (Bharathi *et al.*, 2006; Bharathi *et al.*, 2007), luminescent (Mei *et al.*, 2016) and magnetic materials (Rigamonti *et al.*, 2013; Cejudo *et al.*, 2002; Colacio *et al.*, 1999) and in the construction of MOFs. Copper(II) carboxylates can exhibit various magnetic properties – from the expected paramagnetic behavior (due to the d^9 electronic configuration of the metal ion) to ferromagnetic and antiferromagnetic

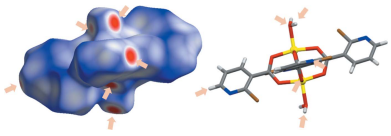

behavior, depending on the ligand coordination modes and copper(II) coordination environments (Rigamonti *et al.*, 2013; Cejudo *et al.*, 2002; Colacio *et al.*, 1999). The metal–metal interaction in copper(II) carboxylates is also an important factor that can affect their magnetic properties and the structure (Rigamonti *et al.*, 2013; Cejudo *et al.*, 2002; Colacio *et al.*. 1999; Ozarowski *et al.*, 2015; Poppl *et al.*, 2008; Sarma *et al.*, 2008).

Polynuclear copper(II) carboxylates have gained much interest in recent years (Zhu *et al.*, 2010; Zhang *et al.*, 2010; Sheikh *et al.*, 2013), for example the copper(II) metal–organic framework containing benzene-1,3,5-tricarboxylate (HKUST-1) is based on dinuclear paddle-wheel copper(II) moieties, with interesting magnetic properties (Chui *et al.*, 1999; Pichon *et al.*, 2007; Furukawa *et al.*, 2008). These paddle-wheel copper(II) moieties have frequently been used in the design of coordination polymers and MOFs as secondary building units (SBU) (Baca *et al.*, 2008; Roubeau & Clerac, 2008; Bai *et al.*, 2008).

Nicotinic acid has been widely used as a complexing agent for various metal ions and many crystal structures of its metal complexes (almost 900) have been reported and deposited in the Cambridge Structural Database (CSD, Version 5.40, searched October 2019; Groom *et al.*, 2016). However, metal complexes of nicotinic acid derivatives have been much less explored. For example, no metal complexes of 2-bromonicotinic acid (2-BrnicH) have been reported so far.

Our goal was to prepare 2-bromonicotinate copper(II) complexes for the above-mentioned significance of copper(II) carboxylates. The syntheses were carried out in aqueous solution to ensure that water molecules (either coordinated and/or hydrated) would be present in their crystal structures, enabling the formation of hydrogen-bonded frameworks. Furthermore, we wanted to explore the type and occurrence of hydrogen bond motifs within the obtained frameworks.

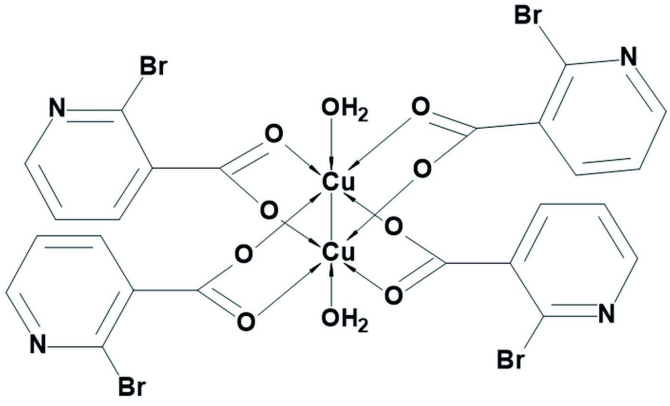

In this work, we report the synthesis and characterization of the first metal complex with 2-bromonicotinic acid – a dinuclear paddle-wheel copper(II) cluster, $[Cu(H_2O)(2\text{-Brnic})_2]_2$ (**1**). Although similar dinuclear paddle-wheel copper(II) carboxylates with coordinated water molecules in the axial positions are well-established and have been extensively studied, there are only a few examples of such compounds that are analogous to **1**, containing nicotinate

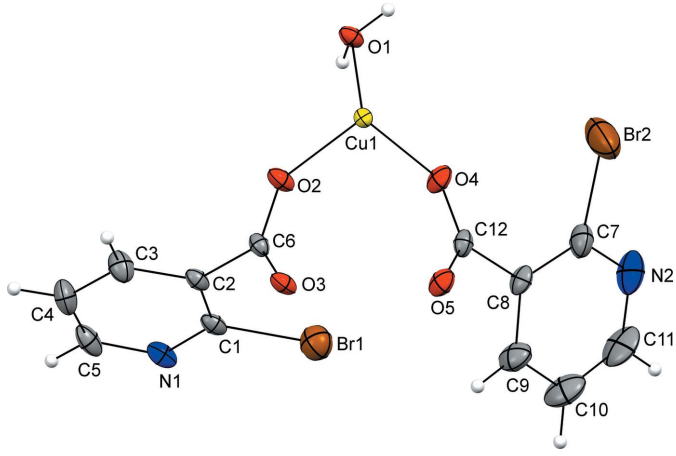

Figure 1
The asymmetric unit of **1**, with the atomic numbering scheme. The displacement ellipsoids are drawn at the 40% probability level.

derivatives [2-chloronicotinate, 2-methoxynicotinate, 2-ethoxynicotinate and 2-(naphthalen-2-ylmethylsulfanyl)nicotinate] as carboxylates (Moncol *et al.*, 2007; Jun, Lu *et al.*, 2013; Jun, Wei-Ping *et al.*, 2013; Adhikari *et al.*, 2016).

2. Structural commentary

The asymmetric unit of **1** consists of a copper(II) ion coordinated by a water molecule and by two deprotonated *O*-monodentate 2-bromonicotinate ligands (Fig. 1). The coordination environment of the copper(II) ion can be described as a distorted square pyramid as τ amounts to 0 [$\tau = (\alpha - \beta)/60°$ (α and β are the largest angles), $\tau = 0$ for an ideal square pyramid and 1 for an ideal trigonal bipyramid; Addison *et al.*, 1984]. The basal plane of the pyramid is defined by four carboxylate O atoms [O2, O4, O3^{i} and O5^{i}; symmetry code: (i) $-x+1, -y+2, -z+1$] from four 2-bromonicotinate ligands while its apical position is occupied by the aqua atom O1 (Fig. 2). The two symmetry-related copper(II) ions are connected into a centrosymmetric paddle-wheel dinuclear cluster [with a Cu···Cu contact length of 2.6470 (11) Å] *via* four *O*,*O*′-bridging 2-bromonicotinate ligands in the *syn–syn*

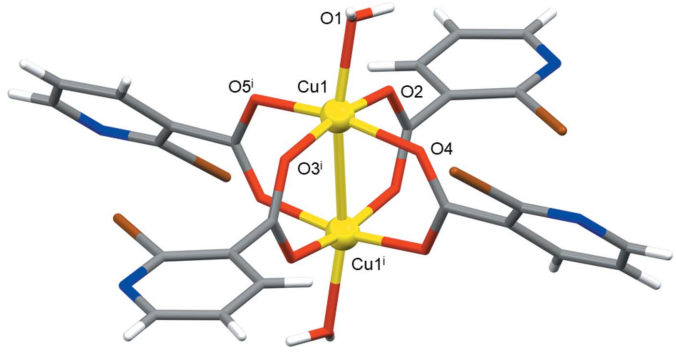

Figure 2
The dinuclear cluster of **1** with selected atoms labeled [symmetry code: (i) $-x+1, -y+2, -z+1$].

Table 1
Hydrogen-bond geometry (Å, °).

D—H···A	D—H	H···A	D···A	D—H···A
O1—H11···O3^{i}	0.82 (1)	2.07 (2)	2.868 (5)	165 (6)
O1—H12···N1^{ii}	0.82 (1)	2.02 (2)	2.816 (6)	166 (6)
C11—H11A···O1^{iii}	0.93	2.51	3.403 (8)	161

Symmetry codes: (i) $x+1, y, z$; (ii) $-x+1, -y+1, -z+1$; (iii) $x, -y+\frac{3}{2}, z+\frac{1}{2}$.

coordination mode (Phetmung & Nucharoen, 2019). This Cu···Cu interaction is slightly longer than the sum of the covalent radii of Cu atoms (2.64 Å; Cordero *et al.*, 2008). The Cu···Cu contact length in **1** is also somewhat longer than those in related paddle-wheel copper(II) clusters with nicotinic acid derivatives (Jun, Lu *et al.*, 2013; Jun, Wei-Ping *et al.*, 2013; Adhikari *et al.*, 2016), but almost equal to that seen in the paddle-wheel copper(II) cluster with 2-chloronicotinic acid (Moncol *et al.*, 2007). The Cu—O_c and Cu—O_w (c = carboxylate, w = water) bond lengths are comparable with literature values (Moncol *et al.*, 2007; Jun, Lu *et al.*, 2013; Jun, Wei-Ping *et al.*, 2013; Adhikari *et al.*, 2016).

The copper(II) ion in **1** is situated nearly at the center of the basal plane with an out-of-plane deviation of 0.209 (2) Å in the direction of the apical Cu1—O1 bond (Fig. 2). The square-pyramidal coordination environment around the copper(II) ion is distorted, as indicated by the angles for the *cis* [88.95 (17)–103.05 (15)°] and *trans* [167.76 (17)–167.80 (15)°] pairs of ligating atoms. There is also a small tetragonal elongation because of the Jahn–Teller effect: Cu1—O1 [2.120 (4)] is somewhat longer than the other four Cu—O bond lengths [1.950 (4)–1.979 (4) Å].

3. Supramolecular features

The extended structure of **1** features strong O—H···O and O—H···N hydrogen bonds, weak C—H···O hydrogen bonds

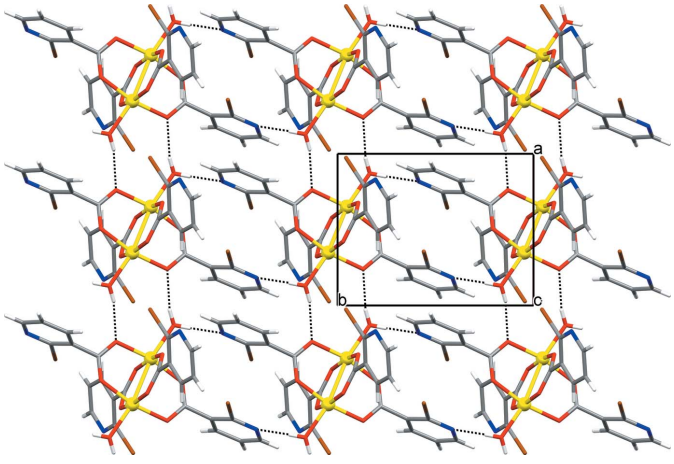

Figure 3
A fragment of the infinite two-dimensional hydrogen-bonded network of **1** viewed along the *c* axis. The cluster molecules are connected by O—H···O and O—H···N hydrogen bonds (represented by the dotted lines) within the network.

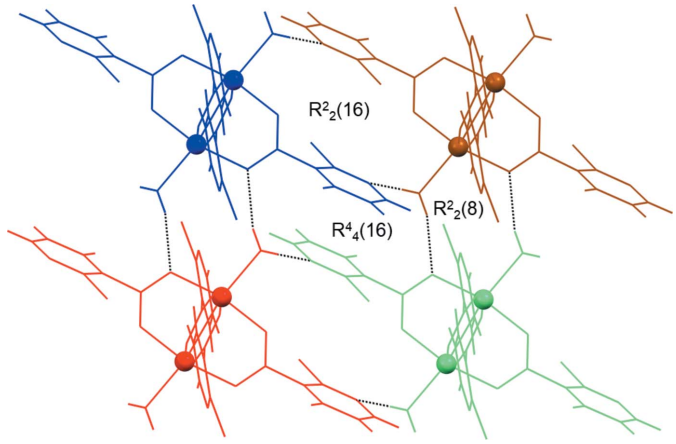

Figure 4
The distinctive hydrogen-bonded ring motifs (represented by dotted lines) found within the layered network of **1**, *viz*. the dimeric $R_2^2(8)$ and $R_2^2(16)$ motifs and the tetrameric $R_4^4(16)$ motif. The various symmetry-related cluster molecules are shown in blue, brown, red and green (see text).

(Table 1) and anion–π interactions [C1—Br1···*Cg*1; where *Cg*1 is the centroid of the pyridine ring N1/C1–C5; Br1···*Cg*1 = 3.629 (2) Å; C1—Br1···*Cg*1 = 103.27 (17)°]. The strong hydrogen bonds link the cluster molecules into an infinite two-dimensional hydrogen-bonded network lying parallel to the (001) plane (Fig. 3), with the anion–π interactions consolidating the layered network. The layers are assembled into a three-dimensional network by the C—H···O bonds.

There are some distinctive hydrogen-bonded ring motifs within the layered network of **1** (Fig. 4). The dimeric $R_2^2(8)$ motif is formed between symmetry-related molecules (indicated in brown and green) *via* two water molecules and two carboxylate O atoms, the dimeric $R_2^2(16)$ motif is formed between symmetry-related molecules (indicated in brown and blue) *via* two water molecules and two pyridine N atoms, while the tetrameric $R_4^4(16)$ motif is formed by symmetry-related molecules (indicated in blue, brown, red and green) *via* two water molecules and two pyridine N atoms (Fig. 4). The water molecules participate in the formation of motifs as both single- and double-proton donors [single in the $R_2^2(8)$ and $R_2^2(16)$ motifs and double in the $R_4^4(16)$ motif], while the carboxylate O and pyridine N atoms participate as single-proton acceptors exclusively. These hydrogen-bonded motifs in **1** are quite different from those in the crystal structures of related paddle-wheel copper(II) clusters with nicotinate derivatives (Jun, Lu *et al.*, 2013; Jun, Wei-Ping *et al.*, 2013; Adhikari *et al.*, 2016). This difference is not surprising in the case of copper(II) clusters with 2-ethoxynicotinate and 2-(naphthalen-2-ylmethylsulfanyl)nicotinate because the presence of water molecules of crystallization drastically affects the crystal packing (Jun, Wei-Ping *et al.*, 2013; Adhikari *et al.*, 2016). The difference in the hydrogen-bonded ring motifs in the case of the copper(II) cluster with 2-methoxynicotinate (Jun, Lu *et al.*, 2013) can be attributed to the different supramolecular arrangement of the cluster molecules, which are connected into a hydrogen-bonded chain, as opposed to a hydrogen-

bonded network in the case of **1**. Furthermore, it seems that the substituents in the nicotinate derivatives (methoxy group *versus* bromine atom) have a great influence on the supramolecular assemblies and on the hydrogen-bond motif types in the respective crystal packings because of the difference in the proton-acceptor abilities of the two substituents.

4. Hirshfeld surface analysis

The Hirshfeld surface analysis of **1** was performed using *CrystalExplorer17.5* (Wolff *et al.*, 2012). Normalized contact distances, d_{norm}, were plotted with standard color settings: regions highlighted in red represent shorter contacts, while longer contacts are shown in blue (Fig. 5). The fingerprint plots show distances from each point on the Hirshfeld surface to the nearest atom inside (d_i) and outside (d_e), and are presented for all contacts and for the contributions of two primary contacts, O—H···O and O—H···N hydrogen bonds (Fig. 6). The percentage contributions of all other selected contacts are presented as a pie chart (Fig. 6).

5. PXRD and thermal analysis

The PXRD analysis was used to confirm the bulk content of **1** (see Fig. S1 in the supporting information). The experimental and calculated PXRD traces of **1** are in very good agreement, confirming the phase purity of **1**.

The thermal stability of **1**, as determined from the TG curve, is up to 140°C (Fig. S2 in the supporting information). The two coordinated water molecules (observed mass loss 3.9%, calculated 3.7%) were released at 176°C (endothermic peak at the DSC curve). The thermal decomposition of **1** continues *via* two consecutive steps (observed mass losses 10.6% and 24.7%) in the temperature range of 190–390°C (exothermic peak at 195°C), which corresponds to the release of approximately one and a half 2-bromonicotinate ligands (calculated mass loss 31.2%). The decomposition finishes with the release of another two 2-bromonicotinate ligands (observed mass loss 46.7%, calculated 41.6%) in the final step (temperature range of 390–600°C). The observed residue (13.3%) at 600°C, remained after total decomposition of **1**, corresponds to CuO. The experimental mass fraction of copper (10.7%) matches nicely with the calculated mass fraction (13.1%).

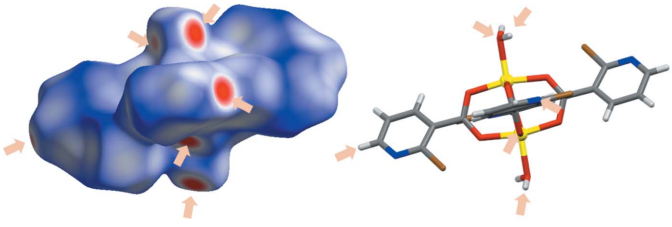

Figure 5
Hirshfeld surfaces on the molecule of **1**. Regions highlighted in red represent shorter contacts, while longer contacts are blue.

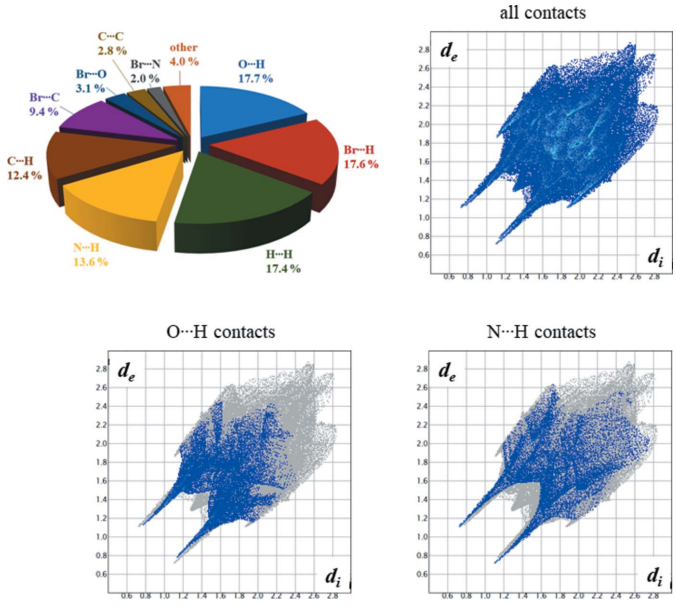

Figure 6
The fingerprint plots showing distances from each point on the Hirshfeld surface to the nearest atom inside (d_i) and outside (d_e), presented for all contacts and for contributions of O—H···O and O—H···N hydrogen bonds in **1**. The percentage contributions of all other selected contacts are shown in a pie chart.

6. Materials and methods

All chemicals for the synthesis were purchased from commercial sources (Merck) and used as received without further purification. The IR spectrum was obtained in the range 4000–400 cm^{-1} on a Perkin–Elmer Spectrum Two^{TM} FTIR-spectrometer in the ATR mode. The PXRD trace was recorded on a Philips PW 1850 diffractometer, Cu $K\alpha$ radiation, voltage 40 kV, current 40 mA, in the angle range 5–50° (2θ) with a step size of 0.02°. Simultaneous TGA/DSC measurements were performed at a heating rate of 10°C min^{-1} in the temperature range 25–800°C, under an oxygen flow of 50 mL min^{-1} on an Mettler–Toledo TGA/DSC 3+ instrument. Approximately 2 mg of the sample was placed in a standard alumina crucible (70 µl).

7. Synthesis and crystallization

2-Bromonicotinic acid (0.0502 g; 0.2485 mmol) was dissolved in distilled water (5 ml) with the addition of a drop of concentrated ammonia solution and then mixed and stirred with an aqueous copper(II) chloride dihydrate solution (0.0220 g; 0.1290 mmol in 2 ml of distilled water). The pH of the obtained solution was adjusted to 6–7 by adding an ammonia solution dropwise. The clear solution was left to evaporate slowly at room temperature for a month until blue crystals of **1**, suitable for X-ray diffraction measurements, were obtained, which were collected by filtration, washed with ethanol and dried *in vacuo*. Yield: 0.0209 g (17%). Selected IR bands (ATR) (ν, cm^{-1}): 3432 [ν(O—H)], 3065 [ν(C—H)],

1623[ν(C═O)), 1385 [ν(C—N)$_{pyridine}$] (Fig. S3, Table S1 in the supporting information).

8. Refinement

Crystal data, data collection and structure refinement details are summarized in Table 2. The C-bound H atoms were placed geometrically (C—H = 0.93 Å) and refined as riding atoms. The water-molecule H atoms were found in difference-Fourier maps and refined with the O—H distances restrained to an average value of 0.82 Å using DFIX and DANG instructions. The constraint U_{iso}(H) = 1.2U_{eq}(carrier) was applied in all cases. The highest difference peak is 1.00 Å away from Br2 and the deepest difference hole is 0.78 Å away from the same atom.

Funding information

This research was supported by a Grant from the Foundation of the Croatian Academy of Sciences and Arts for 2019 and by the University of Split institutional funding.

Table 2
Experimental details.

Crystal data	
Chemical formula	$[Cu(H_2O)(C_6H_3BrNO_2)_2]_2$
M_r	967.13
Crystal system, space group	Monoclinic, $P2_1/c$
Temperature (K)	296
a, b, c (Å)	7.5596 (2), 9.7402 (3), 20.5332 (7)
β (°)	94.345 (3)
V (Å^3)	1507.56 (8)
Z	2
Radiation type	Mo $K\alpha$
μ (mm^{-1})	6.77
Crystal size (mm)	0.59 × 0.42 × 0.33
Data collection	
Diffractometer	Oxford Diffraction Xcalibur2 diffractometer with Sapphire 3 CCD detector
Absorption correction	Multi-scan (*CrysAlis PRO*; Rigaku, 2018)
T_{min}, T_{max}	0.288, 1.000
No. of measured, independent and observed [$I > 2\sigma(I)$] reflections	19205, 2622, 2392
R_{int}	0.028
(sin $\theta/\lambda)_{max}$ (Å^{-1})	0.595
Refinement	
$R[F^2 > 2\sigma(F^2)]$, $wR(F^2)$, S	0.050, 0.134, 1.06
No. of reflections	2622
No. of parameters	205
No. of restraints	3
H-atom treatment	H atoms treated by a mixture of independent and constrained refinement
$\Delta\rho_{max}$, $\Delta\rho_{min}$ (e Å^{-3})	1.34, −2.06

Computer programs: *CrysAlis PRO* (Rigaku, 2018), *SHELXT* (Sheldrick, 2015*a*), *SHELXL2018/3* (Sheldrick, 2015*b*) and *Mercury* (Macrae *et al.*, 2008).

References

Addison, A. W., Rao, T. N., Reedijk, J., van Rijn, J. & Verschoor, G. C. (1984). *J. Chem. Soc. Dalton Trans.* pp. 1349–1356.
Adhikari, S., Sahana, A., Kumari, B., Ganguly, D., Das, S., Banerjee, P. P., Banerjee, G., Chattopadhyay, A., Fondo, M., Matalobos, J. S., Brandão, P., Félix, V. & Das, D. (2016). *New J. Chem.* **40**, 10378–10388.
Baca, S. G., Malaestean, I. L., Keene, T. D., Adams, H., Ward, M. D., Hauser, J., Neels, A. & Decurtins, S. (2008). *Inorg. Chem.* **47**, 11108–11119.
Bai, Y. L., Tao, J., Huang, R. B. & Zheng, L. S. (2008). *Angew. Chem. Int. Ed.* **47**, 5344–5347.
Bharathi, K. S., Rahiman, A. K., Rajesh, K., Sreedaran, S., Aravindan, P. G., Velmurugan, D. & Narayanan, V. (2006). *Polyhedron*, **25**, 2859–2868.
Bharathi, K. S., Sreedaran, S., Rahiman, A. K. & Rajesh, K. (2007). *Polyhedron*, **26**, 3993–4002.
Cejudo, R., Alzuet, G., Borrás, J., Liu-González, M. & Sanz-Ruiz, F. (2002). *Polyhedron*, **21**, 1057–1061.
Chui, S. S.-Y., Lo, S. M.-F., Charmant, J. P. H., Orpen, A. G. & Williams, I. D. (1999). *Science*, **283**, 1148–1150.
Colacio, E., Domínguez-Vera, J. M., Ghazi, M., Kivekäs, R., Klinga, M. & Moreno, J. M. (1999). *Eur. J. Inorg. Chem.* pp. 441–445.
Cordero, B., Gómez, V., Platero-Prats, A. E., Revés, M., Echeverría, J., Cremades, E., Barragán, F. & Alvarez, S. (2008). *Dalton Trans.* pp. 2832–2838.
Fountoulaki, S., Perdih, F., Turel, I., Kessissoglou, D. P. & Psomas, G. (2011). *J. Inorg. Biochem.* **105**, 1645–1655.
Furukawa, H., Kim, J., Ockwig, N. W., O'Keeffe, M. & Yaghi, O. M. (2008). *J. Am. Chem. Soc.* **130**, 11650–11661.
Groom, C. R., Bruno, I. J., Lightfoot, M. P. & Ward, S. C. (2016). *Acta Cryst.* B**72**, 171–179.
Iqbal, M., Ali, S., Muhammad, N. & Sohail, M. (2013). *Polyhedron*, **57**, 83–93.
Jun, W., Lu, L., Wei-Ping, W. & Bin, X. (2013). *J. Chem. Res.* **37**, 287–290.
Jun, W., Wei-Ping, W., Lu, L. & Bin, X. (2013). *J. Mol. Struct.* **1036**, 174–179.
Lim, E.-K., Teoh, S.-G., Goh, S.-M., Ch'ng, C., Ng, C.-H., Fun, H.-K., Rosli, M. M., Najimudin, N., Beh, H.-K., Seow, L.-J., Ismail, N., Ismail, Z., Asmawi, M. Z. & Cheah, Y.-H. (2009). *Polyhedron*, **28**, 1320–1330.
Ma, Y., Cheng, A.-L., Tang, B. & Gao, E.-Q. (2014). *Dalton Trans.* **43**, 13957–13964.
Macrae, C. F., Bruno, I. J., Chisholm, J. A., Edgington, P. R., McCabe, P., Pidcock, E., Rodriguez-Monge, L., Taylor, R., van de Streek, J. & Wood, P. A. (2008). *J. Appl. Cryst.* **41**, 466–470.
Mei, H. X., Zhang, T., Huang, H. Q., Huang, R. B. & Zheng, L. S. (2016). *J. Mol. Struct.* **1108**, 126–133.
Moncol, J., Korabik, M., Segl'a, P., Koman, M., Mikloš, D., Jašková, J., Glowiak, T., Melník, M., Mrozinski, J. & Sundberg, M. R. (2007). *Z. Anorg. Allg. Chem.* **633**, 298–305.
Ozarowski, A., Calzado, C. J., Sharma, R. P., Kumar, S., Jezierska, J., Angeli, C., Spizzo, F. & Ferretti, V. (2015). *Inorg. Chem.* **54**, 11916–11934.
Phetmung, H. & Nucharoen, A. (2019). *Polyhedron*, **173**, 114121. https://doi.org/10.1016/j.poly.2019.114121
Pichon, A., Fierro, C. M., Nieuwenhuyzen, M. & James, S. (2007). *CrystEngComm*, **9**, 449–451.
Poppl, A., Kunz, S., Himsl, D. & Hartmann, M. (2008). *J. Phys. Chem.* **12**, 2678–2684.
Rigaku (2018). *CrysAlis PRO*. Rigaku Inc., Tokyo, Japan.
Rigamonti, L., Carlino, S., Halibi, Y., Demartin, F., Castellano, C., Ponti, A., Pievo, R. & Pasini, A. (2013). *Polyhedron*, **53**, 157–165.
Roubeau, O. & Clérac, R. (2008). *Eur. J. Inorg. Chem.* pp. 4325–4342.
Sarma, R., Karmakar, A. & Baruah, J. B. (2008). *Inorg. Chim. Acta*, **361**, 2081–2086.
Sheikh, J. A., Jena, H. S., Adhikary, A., Khatua, S. & Konar, S. (2013). *Inorg. Chem.* **52**, 9717–9719.
Sheldrick, G. M. (2015*a*). *Acta Cryst.* A**71**, 3–8.
Sheldrick, G. M. (2015*b*). *Acta Cryst.* C**71**, 3–8.

Song, Y. J., Kwak, H., Lee, Y. M., Kim, S. H., Lee, S. H., Park, B. K., Jun, Y. J., Yu, S. M., Kim, C., Kim, S. J. & Kim, Y. (2009). *Polyhedron*, **28**, 1241–1252.
Wolff, S. K., Grimwood, D. J., McKinnon, J. J., Turner, M. J., Jayatilaka, D. & Spackman, M. A. (2012). *CrystalExplorer*. University of Western Australia, Nedlands, Australia
Zhang, J.-Y., Li, X.-B., Wang, K., Ma, Y., Cheng, A.-L. & Gao, E.-Q. (2012). *Dalton Trans.* **41**, 12192–12199.
Zhang, X.-M., Wang, Y.-Q. & Gao, E.-Q. (2010). *Eur. J. Inorg. Chem.* pp. 1249–1254.
Zhu, X., Zhao, J.-W., Li, B.-L., Song, Y., Zhang, Y.-M. & Zhang, Y. (2010). *Inorg. Chem.* **49**, 1266–1270.

supporting information

Acta Cryst. (2020). E**76**, 225-230 [https://doi.org/10.1107/S2056989020000390]

The first coordination compound of deprotonated 2-bromonicotinic acid: crystal structure of a dinuclear paddle-wheel copper(II) complex

Nives Politeo, Mateja Pisačić, Marijana Đaković, Vesna Sokol and Boris-Marko Kukovec

Computing details

Data collection: *CrysAlis PRO* (Rigaku, 2018); cell refinement: *CrysAlis PRO* (Rigaku, 2018); data reduction: *CrysAlis PRO* (Rigaku, 2018); program(s) used to solve structure: SHELXT (Sheldrick, 2015a); program(s) used to refine structure: *SHELXL2018/3* (Sheldrick, 2015b); molecular graphics: *Mercury* (Macrae *et al.*, 2008) and *CrystalExplorer17.5* (Wolff *et al.*, 2012); software used to prepare material for publication: *SHELXL2018/3* (Sheldrick, 2015b).

Tetrakis(*μ*-2-bromonicotinato-*κ*^{2}*O*:*O*′)bis[aquacopper(II)](*Cu*—*Cu*)

Crystal data

$[Cu_2(C_6H_3BrNO_2)_4(H_2O)_2]$
M_r = 967.13
Monoclinic, $P2_1/c$
a = 7.5596 (2) Å
b = 9.7402 (3) Å
c = 20.5332 (7) Å
β = 94.345 (3)°
V = 1507.56 (8) Å^3
Z = 2
$F(000)$ = 932
D_x = 2.131 Mg m^{-3}
Mo $K\alpha$ radiation, λ = 0.71073 Å
Cell parameters from 7938 reflections
θ = 4.6–32.5°
μ = 6.77 mm^{-1}
T = 296 K
Prism, green–blue
0.59 × 0.42 × 0.33 mm

Data collection

Oxford Diffraction Xcalibur2 diffractometer with Sapphire 3 CCD detector
ω–scan
Absorption correction: multi-scan (CrysAlisPro; Rigaku, 2018)
T_{min} = 0.288, T_{max} = 1.000
19205 measured reflections
2622 independent reflections
2392 reflections with $I > 2\sigma(I)$
R_{int} = 0.028
θ_{max} = 25.0°, θ_{min} = 4.3°
h = −8→8
k = −11→11
l = −24→24

Refinement

Refinement on F^2
Least-squares matrix: full
$R[F^2 > 2\sigma(F^2)]$ = 0.050
$wR(F^2)$ = 0.134
S = 1.06
2622 reflections
205 parameters
3 restraints
Primary atom site location: dual
Hydrogen site location: mixed
H atoms treated by a mixture of independent and constrained refinement
$w = 1/[\sigma^2(F_o^2) + (0.0666P)^2 + 10.4972P]$ where $P = (F_o^2 + 2F_c^2)/3$
$(\Delta/\sigma)_{max}$ = 0.001
$\Delta\rho_{max}$ = 1.34 e Å^{-3}
$\Delta\rho_{min}$ = −2.06 e Å^{-3}

Special details

Geometry. All esds (except the esd in the dihedral angle between two l.s. planes) are estimated using the full covariance matrix. The cell esds are taken into account individually in the estimation of esds in distances, angles and torsion angles; correlations between esds in cell parameters are only used when they are defined by crystal symmetry. An approximate (isotropic) treatment of cell esds is used for estimating esds involving l.s. planes.

Fractional atomic coordinates and isotropic or equivalent isotropic displacement parameters (Å²)

	x	*y*	*z*	U_{iso}*/U_{eq}
Cu1	0.65135 (8)	0.95254 (6)	0.48054 (3)	0.0136 (2)
Br1	0.35523 (10)	0.55987 (8)	0.58074 (4)	0.0462 (2)
Br2	0.97277 (15)	0.95629 (13)	0.67690 (5)	0.0838 (4)
N1	0.1831 (6)	0.4145 (5)	0.4818 (3)	0.0259 (10)
N2	0.8306 (9)	0.8063 (7)	0.7703 (3)	0.0518 (16)
O1	0.8705 (5)	0.8353 (4)	0.45349 (18)	0.0201 (8)
H11	0.969 (4)	0.857 (5)	0.469 (3)	0.024*
H12	0.852 (7)	0.758 (3)	0.466 (3)	0.024*
O2	0.4953 (5)	0.7928 (4)	0.4598 (2)	0.0251 (8)
O3	0.2397 (5)	0.8692 (4)	0.49343 (19)	0.0232 (8)
O4	0.6771 (5)	0.8938 (4)	0.57194 (17)	0.0265 (9)
O5	0.4213 (5)	0.9715 (4)	0.60518 (18)	0.0278 (9)
C1	0.2511 (7)	0.5362 (5)	0.4956 (3)	0.0214 (11)
C2	0.2524 (6)	0.6442 (5)	0.4517 (3)	0.0192 (11)
C3	0.1765 (8)	0.6213 (6)	0.3893 (3)	0.0318 (13)
H3	0.172615	0.691086	0.358327	0.038*
C4	0.1065 (9)	0.4933 (7)	0.3734 (3)	0.0361 (14)
H4	0.056199	0.474885	0.331615	0.043*
C5	0.1132 (8)	0.3943 (6)	0.4210 (3)	0.0314 (14)
H5	0.066424	0.308183	0.410259	0.038*
C6	0.3360 (7)	0.7797 (5)	0.4701 (2)	0.0186 (11)
C7	0.7871 (9)	0.8618 (7)	0.7123 (3)	0.0367 (15)
C8	0.6168 (8)	0.8574 (6)	0.6809 (3)	0.0258 (12)
C9	0.4876 (9)	0.7953 (8)	0.7142 (3)	0.0402 (16)
H9	0.370816	0.793989	0.696302	0.048*
C10	0.5309 (12)	0.7351 (9)	0.7740 (4)	0.054 (2)
H10	0.445567	0.689641	0.796168	0.065*
C11	0.7019 (13)	0.7440 (9)	0.7997 (3)	0.058 (2)
H11A	0.730394	0.704053	0.840298	0.069*
C12	0.5703 (7)	0.9133 (5)	0.6139 (2)	0.0211 (11)

Atomic displacement parameters (Å²)

	U^{11}	U^{22}	U^{33}	U^{12}	U^{13}	U^{23}
Cu1	0.0134 (3)	0.0128 (3)	0.0144 (3)	0.0004 (2)	0.0001 (2)	0.0006 (2)
Br1	0.0477 (4)	0.0450 (4)	0.0450 (4)	−0.0018 (3)	−0.0018 (3)	0.0041 (3)
Br2	0.0700 (7)	0.1137 (9)	0.0637 (6)	−0.0456 (6)	−0.0206 (5)	0.0186 (6)
N1	0.019 (2)	0.014 (2)	0.045 (3)	0.0007 (18)	0.003 (2)	0.000 (2)
N2	0.066 (4)	0.057 (4)	0.029 (3)	0.007 (3)	−0.021 (3)	0.008 (3)

O1	0.0135 (17)	0.0172 (18)	0.030 (2)	0.0008 (14)	0.0027 (15)	−0.0025 (16)
O2	0.0172 (19)	0.0185 (19)	0.040 (2)	−0.0033 (14)	0.0033 (16)	−0.0058 (16)
O3	0.0155 (18)	0.0173 (18)	0.037 (2)	−0.0026 (14)	0.0034 (16)	−0.0043 (16)
O4	0.031 (2)	0.033 (2)	0.0157 (18)	0.0089 (17)	−0.0009 (16)	0.0044 (16)
O5	0.032 (2)	0.033 (2)	0.0184 (19)	0.0068 (18)	−0.0004 (16)	0.0049 (16)
C1	0.014 (2)	0.017 (3)	0.033 (3)	0.001 (2)	0.003 (2)	−0.001 (2)
C2	0.015 (2)	0.014 (2)	0.029 (3)	−0.0006 (19)	0.001 (2)	−0.001 (2)
C3	0.037 (3)	0.023 (3)	0.034 (3)	−0.005 (2)	−0.007 (3)	0.004 (2)
C4	0.036 (3)	0.032 (3)	0.038 (3)	−0.005 (3)	−0.011 (3)	−0.009 (3)
C5	0.024 (3)	0.017 (3)	0.051 (4)	−0.002 (2)	−0.005 (3)	−0.008 (3)
C6	0.018 (3)	0.016 (3)	0.021 (3)	−0.003 (2)	−0.003 (2)	0.003 (2)
C7	0.048 (4)	0.038 (3)	0.023 (3)	−0.004 (3)	−0.008 (3)	0.001 (3)
C8	0.037 (3)	0.025 (3)	0.015 (3)	0.005 (2)	−0.003 (2)	0.005 (2)
C9	0.045 (4)	0.048 (4)	0.027 (3)	0.003 (3)	0.005 (3)	0.012 (3)
C10	0.071 (5)	0.059 (5)	0.034 (4)	0.010 (4)	0.015 (4)	0.022 (3)
C11	0.089 (6)	0.060 (5)	0.024 (3)	0.007 (5)	0.002 (4)	0.023 (3)
C12	0.031 (3)	0.015 (2)	0.017 (3)	−0.001 (2)	−0.003 (2)	0.000 (2)

Geometric parameters (Å, º)

Cu1—O5^{i}	1.950 (4)	O5—C12	1.261 (7)
Cu1—O4	1.958 (4)	C1—C2	1.386 (8)
Cu1—O3^{i}	1.978 (4)	C2—C3	1.381 (8)
Cu1—O2	1.979 (4)	C2—C6	1.499 (7)
Cu1—O1	2.120 (4)	C3—C4	1.384 (9)
Cu1—Cu1^{i}	2.6470 (11)	C3—H3	0.9300
Br1—C1	1.875 (6)	C4—C5	1.371 (9)
Br2—C7	1.870 (7)	C4—H4	0.9300
N1—C1	1.314 (7)	C5—H5	0.9300
N1—C5	1.334 (8)	C7—C8	1.396 (9)
N2—C7	1.326 (8)	C8—C9	1.374 (9)
N2—C11	1.331 (11)	C8—C12	1.496 (7)
O1—H11	0.815 (10)	C9—C10	1.378 (9)
O1—H12	0.815 (10)	C9—H9	0.9300
O2—C6	1.245 (6)	C10—C11	1.362 (12)
O3—C6	1.254 (6)	C10—H10	0.9300
O4—C12	1.239 (7)	C11—H11A	0.9300
O5^{i}—Cu1—O4	167.76 (17)	C2—C3—C4	119.2 (6)
O5^{i}—Cu1—O3^{i}	89.64 (17)	C2—C3—H3	120.4
O4—Cu1—O3^{i}	89.35 (17)	C4—C3—H3	120.4
O5^{i}—Cu1—O2	88.95 (17)	C5—C4—C3	118.3 (6)
O4—Cu1—O2	89.47 (17)	C5—C4—H4	120.9
O3^{i}—Cu1—O2	167.80 (15)	C3—C4—H4	120.9
O5^{i}—Cu1—O1	98.06 (16)	N1—C5—C4	123.6 (5)
O4—Cu1—O1	94.05 (15)	N1—C5—H5	118.2
O3^{i}—Cu1—O1	103.05 (15)	C4—C5—H5	118.2
O2—Cu1—O1	89.15 (15)	O2—C6—O3	126.2 (5)

O5^{i}—Cu1—Cu1^{i}	87.08 (12)	O2—C6—C2	116.3 (5)
O4—Cu1—Cu1^{i}	80.69 (12)	O3—C6—C2	117.5 (4)
O3^{i}—Cu1—Cu1^{i}	87.92 (11)	N2—C7—C8	124.0 (6)
O2—Cu1—Cu1^{i}	79.91 (11)	N2—C7—Br2	114.0 (5)
O1—Cu1—Cu1^{i}	167.85 (11)	C8—C7—Br2	121.9 (5)
C1—N1—C5	117.1 (5)	C9—C8—C7	116.7 (5)
C7—N2—C11	117.0 (7)	C9—C8—C12	119.4 (5)
Cu1—O1—H11	118 (4)	C7—C8—C12	123.9 (5)
Cu1—O1—H12	105 (4)	C8—C9—C10	120.1 (7)
H11—O1—H12	107 (4)	C8—C9—H9	120.0
C6—O2—Cu1	127.8 (3)	C10—C9—H9	120.0
C6—O3—Cu1^{i}	118.1 (3)	C11—C10—C9	118.3 (7)
C12—O4—Cu1	126.8 (3)	C11—C10—H10	120.9
C12—O5—Cu1^{i}	119.1 (3)	C9—C10—H10	120.9
N1—C1—C2	124.5 (5)	N2—C11—C10	123.9 (6)
N1—C1—Br1	116.2 (4)	N2—C11—H11A	118.1
C2—C1—Br1	119.3 (4)	C10—C11—H11A	118.1
C3—C2—C1	117.3 (5)	O4—C12—O5	126.3 (5)
C3—C2—C6	120.9 (5)	O4—C12—C8	117.6 (5)
C1—C2—C6	121.8 (5)	O5—C12—C8	116.0 (5)
C5—N1—C1—C2	1.0 (8)	C11—N2—C7—C8	−0.5 (11)
C5—N1—C1—Br1	−178.0 (4)	C11—N2—C7—Br2	176.5 (6)
N1—C1—C2—C3	0.0 (8)	N2—C7—C8—C9	2.4 (10)
Br1—C1—C2—C3	179.0 (4)	Br2—C7—C8—C9	−174.4 (5)
N1—C1—C2—C6	−178.5 (5)	N2—C7—C8—C12	−176.5 (6)
Br1—C1—C2—C6	0.5 (7)	Br2—C7—C8—C12	6.7 (9)
C1—C2—C3—C4	−1.0 (9)	C7—C8—C9—C10	−3.3 (10)
C6—C2—C3—C4	177.6 (6)	C12—C8—C9—C10	175.6 (6)
C2—C3—C4—C5	0.9 (10)	C8—C9—C10—C11	2.6 (12)
C1—N1—C5—C4	−1.1 (9)	C7—N2—C11—C10	−0.4 (13)
C3—C4—C5—N1	0.2 (10)	C9—C10—C11—N2	−0.7 (14)
Cu1—O2—C6—O3	3.4 (8)	Cu1—O4—C12—O5	2.3 (8)
Cu1—O2—C6—C2	−177.5 (3)	Cu1—O4—C12—C8	179.3 (4)
Cu1^{i}—O3—C6—O2	−2.0 (7)	Cu1^{i}—O5—C12—O4	−2.9 (8)
Cu1^{i}—O3—C6—C2	178.9 (3)	Cu1^{i}—O5—C12—C8	−179.9 (4)
C3—C2—C6—O2	−87.8 (6)	C9—C8—C12—O4	−138.3 (6)
C1—C2—C6—O2	90.7 (6)	C7—C8—C12—O4	40.6 (8)
C3—C2—C6—O3	91.3 (6)	C9—C8—C12—O5	39.0 (8)
C1—C2—C6—O3	−90.2 (6)	C7—C8—C12—O5	−142.2 (6)

Symmetry code: (i) −*x*+1, −*y*+2, −*z*+1.

Hydrogen-bond geometry (Å, º)

D—H···*A*	*D*—H	H···*A*	*D*···*A*	*D*—H···*A*
O1—H11···O3^{ii}	0.82 (1)	2.07 (2)	2.868 (5)	165 (6)

O1—H12···N1^{iii}	0.82 (1)	2.02 (2)	2.816 (6)	166 (6)
C11—H11*A*···O1^{iv}	0.93	2.51	3.403 (8)	161

Symmetry codes: (ii) *x*+1, *y*, *z*; (iii) −*x*+1, −*y*+1, −*z*+1; (iv) *x*, −*y*+3/2, *z*+1/2.